Nonlinear/Non-Gaussian Friction Estimation and Compensation using Particle Filter

M2018SC009 Yoshihiko SUZUKI
Supervisor Gan CHEN

1 Introduction

Friction with strong nonlinearity and time-dependency on some operating conditions deteriorates the performance of positioning control. The aim of this thesis is the improvement of the performance by a controller consisting of an error-feedback controller and a compensator for nonlinear/non-Gaussian friction. The friction is modeled by the LuGre model[1], which approximates a contact surface as bristles meshing with two brushes. The LuGre model with fewer parameters includes many frictional characteristics, e.g., the Stribeck effect, time-lag (Hysteresis), the pre-sliding-regime and the sliding regime. The model and its parameters depend on these operating conditions. We consider these parameters are estimated by nonlinear filter in real-time. The particle filter[2] is a nonlinear filter based on the Monte Carlo method and uses many random numbers and particles, which are the samples of state vector. The particle filter represents any distribution as a histogram using many particles. Consequently, the particle filter can accurately estimate the nonlinear/non-Gaussian friction. We propose a method with some modifications improving the accuracy of the particle filter. We optimize the covariances of the system noise and the observation noise by using the Nelder Mead method[3], which is a parameter optimization by moving a polytope in search space. We find more appropriate sampling time and improve the performance. The minimum sampling time does not provide the best performance for the particle filter in real-time, in contrast to standard observers. The experiments by an X-Y table illustrate the effectiveness of the proposed method with these modifications.

2 Modeling

The models of a ball screw system and a nonlinear friction are described in this chapter.

2.1 Modeling of Ball Screw System

A ball screw system is composed of a motor, a ball screw, a table, and a guide rail. The table motion is disturbed by nonlinear friction between the table and the guide rail. A position of the table is p, an angle of the motor is θ, an angular velocity is ω, an angular acceleration is a, a motor torque is τ, a mass of the table is M, an inertia moment of the rotating system is J, a viscous friction coefficient is σ_2, a lead of the ball screw is L, and a nonlinear friction is F_{nl}. Since the ball screw is stiff, suppose that its strain is negligible, i.e., $p = L\theta$($\frac{d}{dt}p = L\omega$, $\frac{d^2}{dt^2}p = La$). Then, a dynamical model of the ball screw system is derived as (1).

$$(J + L^2M)a = -L(\sigma_2 L\omega + F_{nl}) + \tau \tag{1}$$

Let $x = [\theta\ \omega]^{\mathrm{T}}$ be state vector, then a state-space representation of the ball screw system is obtained as (2).

$$\begin{cases} \frac{d}{dt}x &= Ax + Bu - BLF_{nl} \\ y &= Cx \end{cases}, \tag{2}$$

$$A = \begin{bmatrix} 0 & 1 \\ 0 & -\frac{L^2\sigma_2}{J+L^2M} \end{bmatrix}, B = \begin{bmatrix} 0 \\ \frac{1}{J+L^2M} \end{bmatrix}, C = [1 \quad 0],$$

where $u = \tau$ is an input, $y = \theta$ is an output.

2.2 Modeling of Nonlinear Friction

We consider to increase the performance of the positioning control using a friction-model-based compensator. The nonlinear friction is modeled by the LuGre model[1], because the model captures some characteristics of the nonlinear friction by fewer parameters. The model represents a contact surface as an aggregation of bristles, and represents a transition from the pre-sliding regime (the time region until a stiction reaches the maximum stiction) to the sliding regime (the time region after reaching the maximum stiction) as a dynamics of the bristle. A mathematical expression of the LuGre model is given as follows:

$$F_{nl} = \sigma_0 z + \sigma_1 \frac{d}{dt}z, \tag{3}$$

$$\frac{d}{dt}z = L\omega - \sigma_0 \frac{L|\omega|}{g(\omega)}z, \tag{4}$$

$$g(\omega) = (F_c + (F_s - F_c)\exp(-\frac{L|\omega|}{v_s})) > 0, \tag{5}$$

where z is a position of the bristle, σ_0 is a spring coefficient of the bristle, σ_1 is a damper coefficient of the bristle, F_C is a Coulomb friction, F_S is a maximum stiction, and v_s is a Stribeck velocity. Equation (3) represents the nonlinear friction F_{nl} by a damper and a spring of the bristle. Equations (4) and (5) are the dynamics of the bristle and the Stribeck curve function, respectively. Equations (3) - (5) are used to estimate and compensate the nonlinear friction.

2.3 Equation for Estimation of Friction

The nonlinear friction is estimated through the estimation for the frictional parameter of the LuGre model. In this section, the nonlinear equation used for the estimation of the nonlinear friction is derived. In this study, particle filter is used for an estimation method of the nonlinear friction (the particle filter will be described later in detail). The improvement of computational efficiency for particle filter leads to improving the estimation accuracy. For this purpose, three parameters F_S, F_C and v_s in the function $g(\omega)$ are estimated collectively as one parameter g_p rather than identifying each of them. Then, the parameter g_p is regarded as constant ($\frac{d}{dt}g_p = 0$). Let $x_L(t) = [x_1(t)\ x_2(t)\ x_3(t)\ x_4(t)]^{\mathrm{T}} = [\theta(t)\ \omega(t)\ z(t)\ g_p(t)]^{\mathrm{T}}$ as a state vector, then equation

(2), (3) and (4) leads to the nonlinear system (6).

$$\begin{cases} \frac{d}{dt}\hat{x}_L(t) &= f(\hat{x}_L(t),\ u(t)) \\ \hat{y}_L(t) &= h(\hat{x}_L(t)) \end{cases} \tag{6}$$

$$f(\hat{x}_L(t),\ u(t)) = \begin{bmatrix} \hat{x}_2(t) \\ \frac{-L(\sigma_2 L\hat{x}_2(t)+\hat{F}_{nl}(\hat{x}_L(t))+u(t)}{J+L^2M} \\ L\hat{x}_2(t) - \sigma_0 \frac{L|\hat{x}_2(t)|}{\hat{x}_4(t)}\hat{x}_3(t) \\ 0 \end{bmatrix}$$

$$h(\hat{x}_L(t)) = [1 \quad 0 \quad 0 \quad 0]\,\hat{x}_L(t) = \hat{x}_1(t)$$

$$\begin{aligned} \hat{F}_{nl}(\hat{x}_L(t)) &= \sigma_1 L\hat{x}_2(t) + (\sigma_0 - \sigma_1 \frac{\sigma_0 L|\hat{x}_2(t)|}{\hat{x}_4(t)})\hat{x}_3(t) \\ &= f_{nl}(\hat{x}_2(t),\ \hat{x}_3(t),\ \hat{x}_4(t)) \end{aligned}$$

We estimate the state $\hat{x}_L(t)$ and the nonlinear friction $\hat{F}_{nl}(x_L(t))$ using (6) and the particle filter.

3 Friction Estimation

The parameters of the LuGre model are time-dependent because friction depends on some operating conditions. We estimate the parameters in real-time using the particle filter (PF)[2]. The PF is a filtering method using Monte Carlo simulation with many samples of a state vector called particles. It is known that the PF can estimate the nonlinear/non-Gaussian system with high accuracy. We propose a method to estimate the nonlinear friction using the PF with some modifications to improve the estimation accuracy.

3.1 Particle Filter

An algorithm of the PF is shown as follows[2], where m is a particle size, $x_p^{(i)}(k)$ is an i-th predicted particle at discrete time k, $x_f^{(j)}(k) = [x_{f_1}^{(j)}(t)\ x_{f_2}^{(j)}(t)\ x_{f_3}^{(j)}(t)\ x_{f_4}^{(j)}(t)]^{\mathrm{T}}$ is a j-th filtered particle at k, and $\alpha^{(i)}(k)$ is a weight for the predicted particle $x_p^{(i)}(k)$.

0. Initialization
   Generate particles $x_f^{(j)}(0), j = 1, \cdots, m$. Set $k = 1$.
1. Prediction Step ($i = 1, \cdots, m$)
   First, discretize (6) by the Runge-Kutta method and update $x_f^{(i)}(k-1)$ to $x_p^{(i)}(k)$. Next, generate samples of the system noise $w^{(i)}(k) \sim N(0, Q)$ using random numbers. (Load the random numbers previously stored in memory instead of generating in online to reduce the computation time.) Add the samples to the particles.
   $$x_p^{(i)}(k) \leftarrow x_p^{(i)}(k) + w^{(i)}(k)$$
2. Filtering step ($i = 1, \cdots, m$)
   Evaluate the particle weights by the following function (where $A^{-1}[x]$ means $x^{\mathrm{T}}A^{-1}x$) on the assumption of the observation noise $v \sim N(0, R)$.
   $$\alpha^{(i)}(k) = \exp(-0.5R^{-1}[y(k) - h(x_p^{(i)}(k))])$$
   Normalize the weights.
   $$\tilde{\alpha}^{(i)}(k) = \alpha^{(i)}(k) / \sum_{i=1}^{m} \alpha^{(i)}(k)$$
3. Resampling step ($j = 1, \cdots, m$)
   Find i such that the following conditions proposed in [2]. $\sum_{l=1}^{i-1} \tilde{\alpha}^{(l)}(k) < \xi^{(j)} \le \sum_{l=1}^{i} \tilde{\alpha}^{(l)}(k),\ \xi^{(j)} = \frac{j-0.5}{m}$. Renew $x_f^{(j)}(k) = x_p^{(i)}(k)$.
4. Calculate the mean of the particles and derive the estimated values.
   $\hat{x}_L(k) = \frac{1}{m}\sum_{j=1}^{m} x_f^{(j)}(k)$
   $\hat{F}_{nl}(k) = \frac{1}{m}\sum_{j=1}^{m} f_{nl}(x_{f_2}^{(j)}(k),\ x_{f_3}^{(j)}(k),\ x_{f_4}^{(j)}(k))$
5. Set $k \leftarrow k+1$. Return 1. Prediction step.

The resampling scheme rejects inaccurate particles and increases accurate particles. The resampling scheme is based on the inversion method. The mean calculation of the nonlinear friction is notable. The mean varies with procedures for calculation, e.g., "Insert the mean of the particles into the nonlinear friction equation", and "Calculate the mean of the nonlinear frictions for each particle". In this study, we use the latter because of focusing on the distribution of nonlinear friction.

In the following subsections, we propose modifications to improve the estimation accuracy of the PF and to reduce the computational resources.

3.2 Optimization of Covariance by NMM

We discuss a modification in this section. The estimation accuracy of the PF varies by the covariances of the system noise and the observation noise. Trial and error tunes for these covariances make the PF performance better in many cases, while in this study we adopt the Nelder Mead method (NMM)[3] for a parameter optimization method. The NMM optimizes parameters, by moving a polyhedron (called simplex) in a search space. the discontinuity of the PF and no friction sensor make the optimization of these covariance difficult. Even in such cases, the NMM can optimize because the optimization with the NMM requires only experimental data, not the model or derivative.

Fig. 1 illustrates some experimental results that NMM optimizes the covariances by moving it in the direction of the small objective value as the control error. The vertical axis is the RMS of control error, and the horizontal axis is iterations. In Fig. 1, the RMS of the control error decreases through some iterations.

3.3 Optimization of Sampling Time

Sampling time has a trade-off relationship for particle filter in real-time. The decrease in sampling time causes decreasing the estimation error of PF with the discretization error of the model because PF is a model-based observer. On the other hand, the long sampling time enables us to increase the particle size m and decrease the estimation error with Monte Carlo error in real-time because PF is based on the Monte Carlo method. Hence, the estimation accuracy does not al-

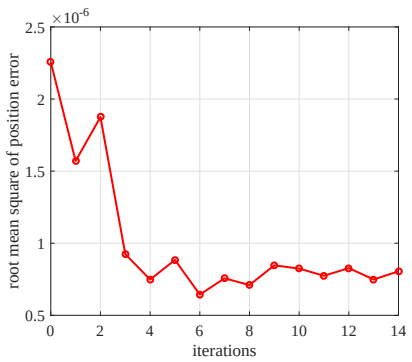

Fig. 1 RMSE decreasing through some iterations

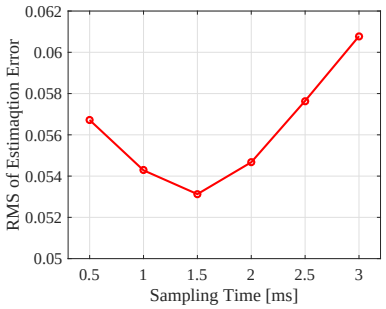

Fig. 2 RMSE values vs. each sampling time Δt

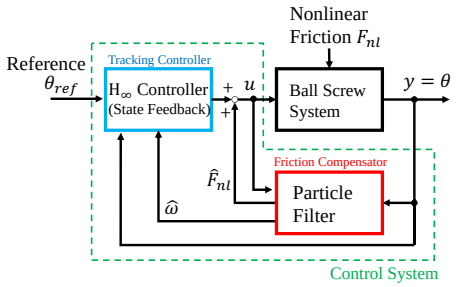

Fig. 3 Diagram of control system

ways improve with decreasing the sampling time. In this study, we find the optimal sampling time by simulating at different sampling times and particle sizes. In simulations, the PF estimates the nonlinear friction in the ball screw controlled by only the feedback controller without a friction compensator in offline. Fig. 2 describes the estimation errors at each sampling time Δt and $1000 \times \Delta t$ particles. As a result, we found the optimal sampling time $\Delta t_{\rm opt} = 1.5$ms with the minimum estimation error.

4 Control System

A servo system is designed for the ball screw system. A derivative of control error between a reference θ_{ref} and the output $y = \theta$ is $\frac{d}{dt}\epsilon = \theta_{ref} - \theta$, a disturbance is $d = LF_{nl}$, an evaluation output is z_e, and weighted matrixes for the evaluation output are C_z, D_z. Let $x_e = [\theta\ \omega\ \epsilon]^{\rm T}$ be a state vector, then an augmented system is obtained as (7).

$$\left\{ \begin{array}{lcl} \frac{d}{dt}x_e &=& A_e x_e + B_e u - B_e d \\ z_e &=& C_z x_e + D_z u \end{array} \right. , \quad A_e = \left[\begin{array}{cc} A & 0 \\ -C & 0 \end{array} \right], \ B_e = \left[\begin{array}{c} B \\ 0 \end{array} \right]. \tag{7}$$

We design a state feedback gain K_∞ that minimizes an H_∞ norm from disturbance d to the evaluation z_e in (7).

A diagram of the control system is as shown in Fig. 3. The control system consists of a feedback structure with H_∞ controller and a friction compensator by the PF. The PF estimates (and compensates) the nonlinear friction occurring in the ball screw system. Since designed to minimize the H_∞ norm from the friction to the control error, the H_∞ controller deals with the estimation error of the PF.

5 Experiments

In this subsection, some experiments show the effectiveness of the proposed method. The nonlinear friction changes greatly at the time when the table motion is reversing. We focus on the transition from the presliding regime to the sliding regime because the friction is strongly nonlinear and non-Gaussian in this region. An apparatus for experiments is an X-Y table. The circular orbit drawn by the X-Y table makes the influence of friction clearly. It draws a circle with a radius of 1.0×10^{-4}m over 8 seconds, in other words, the references of the axis-X and Y are sine wave and cosine wave with frequency 1/8Hz and amplitude 1.0×10^{-4}m, respectively. The resolutions of encoder are approximately 7.6 nm, and sufficiently smaller than the reference. The effectiveness of the proposed method is shown by the comparison among three experiments with three methods: "H_∞ and PF", "H_∞ and UKF", and "H_∞ only". The first method "H_∞ and PF", which is composed of the H_∞ controller and the friction compensator with the PF, is a proposed method as shown in Fig. 3. The second method "H_∞ and UKF" uses the unscented Kalman filter (UKF) instead of the PF. The UKF, which is one of the nonlinear Kalman filters, differs from the PF in the approximation of the PDF. The UKF estimates a state by approximating its distribution as few points called sigma-points. The third method "H_∞ only" uses only the H_∞ controller without friction compensator. The sampling times are set to 1.5ms in the case of "H_∞ and PF", and set to 1.0ms in the others for the best performance. The particle size is 1500.

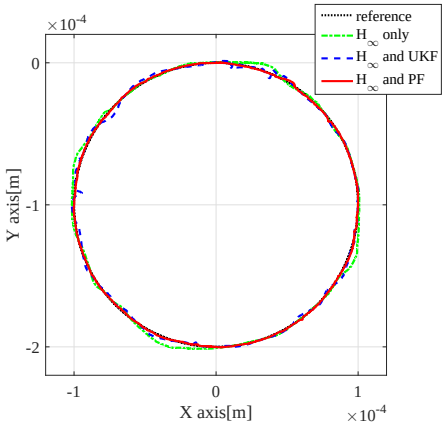

Fig. 4 Experiments results using each controller

5.1 Performance of Control

In this subsection, the control performance is discussed. Fig. 4 shows the trajectories of the table and Fig. 5 describes the errors between the reference and each trajectory. The dotted line is reference, the dash-dot line is the trajectory of the "H_∞ only", the dashed line is of the "H_∞ and UKF", and the solid line is of the "H_∞ and PF". In Fig. 4, the horizontal and vertical axes mean the table deflection of axis-X and Y, respectively. In Fig. 5, the vertical axis indicates the control error, and the horizontal axis means angle. The positive errors indicate that the table is outside the circle, while the negative means inside. The trajectory of the "H_∞ only" in Figs. 4 and 5 shows the quadrant glitches, which are some outward errors at the friction reversing with the table motion. The comparison with "H_∞ only" and "H_∞ and PF" proves that the proposed method compensates the nonlinear friction. The "H_∞ and UKF" in Figs. 4 and 5 show some inward errors

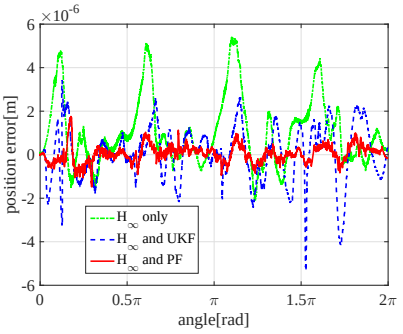

Fig. 5 Tracking error in experiment

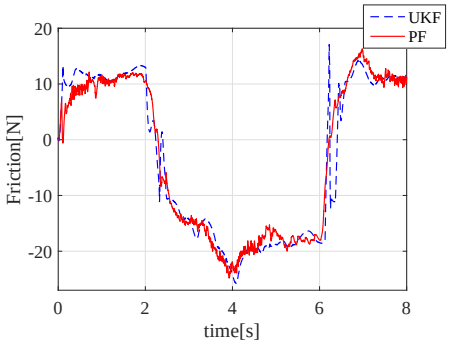

Fig. 6 Estimated friction in experiment

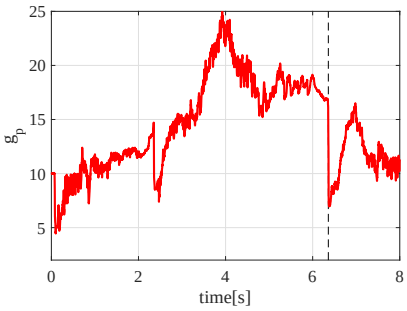

Fig. 7 Time response of $\hat{g}_p$

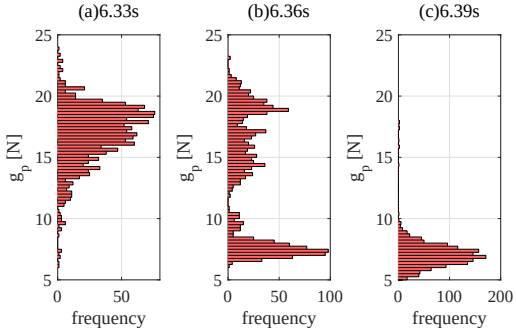

Fig. 8 Particle histograms of $\hat{g}_p$(a)6.33s(b)6.36s(c)6.39s

of the circle without quadrant glitches. The cause of these inward errors is that the UKF over-estimates and over-compensates for the nonlinear friction. This result provides the evidence that the PF more accurately estimates the nonlinear friction than the UKF. (We discuss why the PF accurately estimates the friction in subsection 5.2). The errors quantitatively evaluated as RMS are 4.0×10^{-7} with "H_∞ and PF", 1.3×10^{-6} with "H_∞ and UKF", and 2.4×10^{-6} with "H_∞ only". Thus, the proposed method is the best of them.

5.2 Estimation for Friction

Next, let us consider the estimation accuracy of the PF for the nonlinear/non-Gaussian friction. Fig. 6 depicts the nonlinear frictions estimated by the PF and the UKF in each experiment. In Fig. 6, the vertical axis is the estimated friction [N], and the horizontal axis is time [s]. The solid line and the dashed line show the estimated nonlinear friction by the PF and by the UKF, respectively. (Note that these estimated frictions are from different experiments). The differences in the estimated frictions are observed at the inversion of the friction. The nonlinear friction estimated by the UKF overshot at the point. The inaccurate estimation causes the over-compensation so that the table trajectory is not on the circle but inside as shown in Figs. 4 and 5. The reason is that the PF accurately approximates the non-Gaussian distribution of the nonlinear/non-Gaussian friction as described below. We show the non-Gaussianity of the PF. Fig. 7 illustrates the static-frictional term g_p estimated by the PF. The term g_p rapidly changes from 18N to 7N around 6.36 s while the friction transits from the pre-sliding regime to sliding regime. Fig. 8 (a), (b) and (c) illustrate three particle distributions of the PF right before, during and right after the characteristic g_p varies, respectively. In Fig. 8, the vertical axis means the static-frictional term, and the horizontal axis indicates frequency. Fig. 8 (a) and (c) show the Gaussian distributions with mean 18N and 7N, respectively, while in Fig. 8 (b), the non-Gaussian distribution with two peaks centered at 18N and 7N is observed. Consequently, the PF is to estimate the nonlinear and non-Gaussian friction.

6 Conclusion

The purpose of this thesis is a precise positioning control by a friction compensator. The friction in the X-Y table is estimated by the PF and compensated. In this study, we propose a method with three modeifications to improve the estimation accuracy of the PF. The NMM optimizes the covariances of the system noise and the observation noise. The most appropriate sampling time considering the trade-off relationship is provided by simulations. The experimental results and the comparisons show: the validity of the PF for the nonlinear/non-Gaussian friction and the effectiveness of the proposed method with three modifications.

References

[1] C. Canudas de Wit, H. Olsson, K. J. Åström, and P. Lischinsky, "A New Model for Control of Systems with Friction," *IEEE Transactions on Automatic Control*, Vol. 40, No. 3, pp. 419-425, 1995

[2] G. Kitagawa, "Monte Carlo Filter and Smoother for Non-Gaussian Nonlinear State Space Models," *Journal of Computational and Graphical Statistics*, Vol. 5, No. 1, pp. 1-25, 1996

[3] J. A. Nelder and R. Mead, "A Simplex Method for Function Minimization," *The computer Journal*, Vol. 7, Issue 4, pp. 308-313, 1965.